Non-Innocent Ligands

International Edition: DOI: 10.1002/anie.201507302
German Edition: DOI: 10.1002/ange.201507302

Tripyrrindione as a Redox-Active Ligand: Palladium(II) Coordination in Three Redox States

*Ritika Gautam, Jonathan J. Loughrey, Andrei V. Astashkin, Jason Shearer, and Elisa Tomat**

Abstract: *The tripyrrin-1,14-dione scaffold of urinary pigment uroerythrin coordinates divalent palladium as a planar tridentate ligand. Spectroscopic, structural and computational investigations reveal that the tripyrrindione ligand binds as a dianionic radical, and the resulting complex is stable at room temperature. One-electron oxidation and reduction reactions do not alter the planar coordination sphere of palladium(II) and lead to the isolation of two additional complexes presenting different redox states of the ligand framework. Unaffected by stability problems common to tripyrrolic fragments, the tripyrrindione ligand offers a robust platform for ligand-based redox chemistry.*

Redox-active (or redox non-innocent) ligands in coordination compounds can act as electron reservoirs, thereby extending opportunities for multi-electron transformations beyond the redox chemistry of the metal center(s). The design and study of such ligands is key to the engineering of new catalytic systems featuring additional pathways for redox reactivity.[1–4] Within biological catalysts, the storage and release of redox equivalents on tetrapyrrolic ligands is critical in numerous heme enzymes including catalases and cytochrome P450 monooxygenases. Synthetic tetrapyrroles, such as porphyrins,[5] corroles,[6–8] and bilins,[9,10] as well as expanded porphyrin macrocycles[11–15] and tetradentate bis(phenolate)-dipyrrins,[16] display rich ligand-based redox chemistry. In contrast, the stabilization of unpaired electrons is not well documented for smaller dipyrrolic and tripyrrolic fragments. Herein, we describe the one-electron redox chemistry of a stable tripyrrindione framework in palladium(II) complexes.

Conjugated tripyrroles are attractive ligand platforms, likely inheriting the exquisite electronic tunability of porphyrins while allowing access to the metal center for additional coordination in the plane of the ligand. The coordination chemistry of tripyrroles, however, suffers from limited stability of the ligands and complicated redox chemistry in the presence of transition metals (often leading to ligand deterioration).[17] For instance, tripyrrins (Scheme 1) are typically stable as protonated salts in neat trifluoroacetic acid, but decompose rapidly in the presence of nucleophiles.[18] In addition, tripyrrane[19] and tripyrrin-1-one[20] scaffolds, as well as pyrrolyldipyrrin prodigiosin[21,22] (Scheme 1), undergo oxidative ligand degradation in the presence of Cu^{II} ions.

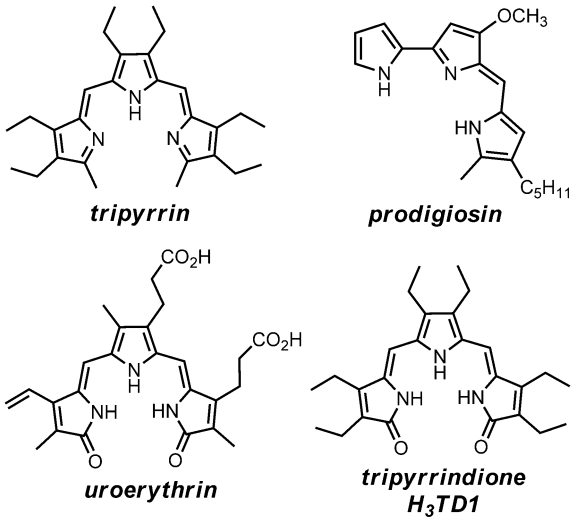

Scheme 1. Examples of naturally occurring and synthetic tripyrrolic scaffolds.

A tripyrrolic motif is found in the structure of ubiquitous urinary pigment uroerythrin (Scheme 1), which was first isolated in 1975 from the pool of pigments excreted in human urine and generically known as urochrome.[23,24] We reasoned that the tripyrrin-1,14-dione scaffold of this physiological product of heme degradation could serve as a stable platform for metal coordination. In addition, the ability of tetrapyrrolic bilindione (i.e., an analog of heme metabolite biliverdin) to stabilize ligand-based radicals[9,25] prompted us to consider tripyrrindiones as potential redox-active ligands.

The most stable *syn-Z* configuration[26] (shown in Scheme 1) of the extended π system of tripyrrindione appears well suited for metal binding, and a color change upon Zn^{II} addition was recorded for both natural uroerythrin[23] and synthetic hexaethyl tripyrrindione H_3TD1;[27] nevertheless, the only reported complexes of these ligands are fluorescent difluorylboryl (BODIPY-type) compounds.[27] We observed that addition of palladium(II) acetate (1.2 equiv) to a solution of H_3TD1 in tetrahydrofuran under ambient conditions led to a gradual change in color from deep red to dark blue. Crystallization and analysis of the product confirmed the coordination of a palladium center.

[*] R. Gautam, Dr. J. J. Loughrey, Dr. A. V. Astashkin, Prof. Dr. E. Tomat
Department of Chemistry and Biochemistry, University of Arizona
1306 E. University Blvd., Tucson AZ 85721 (USA)
E-mail: tomat@email.arizona.edu
Prof. Dr. J. Shearer
Department of Chemistry, University of Nevada
Reno NV 89577 (USA)

Supporting information for this article is available on the WWW under http://dx.doi.org/10.1002/anie.201507302.

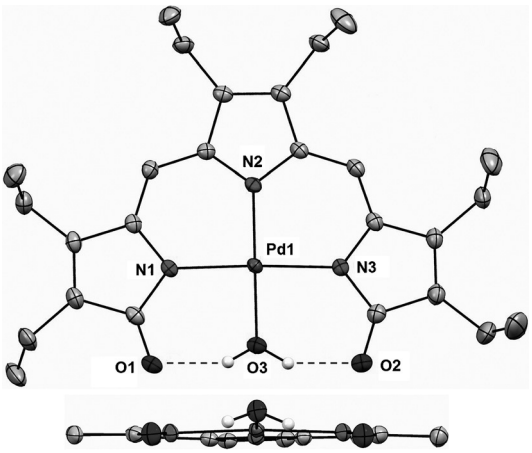

Figure 1. Crystal structure (top and side views) of [Pd(TD1•)(H_2O)] showing a partial atom labeling scheme and hydrogen-bonding interactions (dashed lines). Carbon-bound hydrogen atoms in calculated positions are omitted for clarity. In the side view, peripheral ethyl groups are not shown. Thermal displacement ellipsoids are set at the 50% probability level (CCDC 1400990).

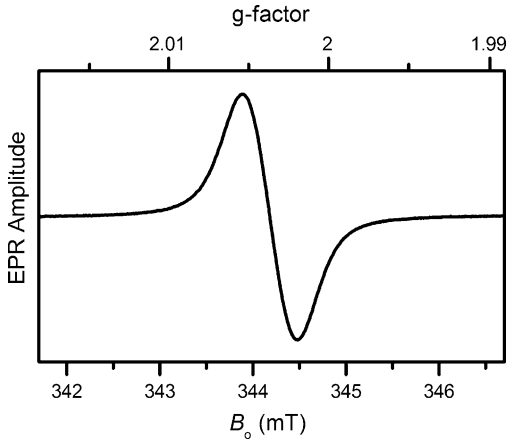

Figure 2. EPR spectrum of 1 mM [Pd(TD1•)(H_2O)] in liquid toluene solution at 296 K. Experimental conditions: microwave (mw) frequency, 9.652 GHz; mw power, 200 μW; magnetic field modulation amplitude, 30 μT.

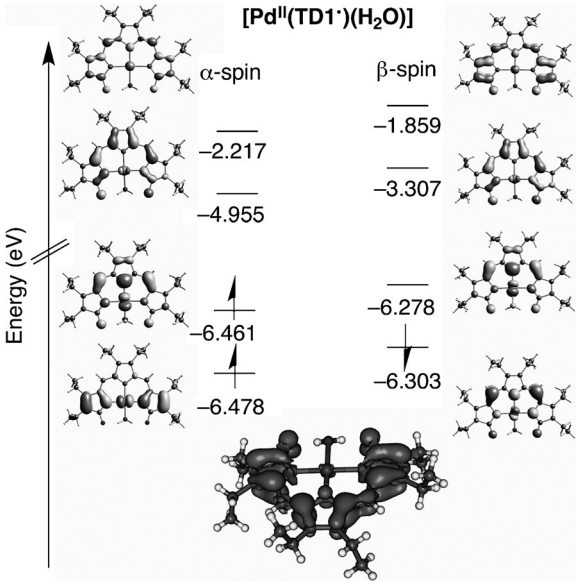

Figure 3. Partial MO diagram for [Pd(TD1•)(H_2O)] with corresponding isosurface plots (top) and spin density plot (bottom).

The crystal structure of the coordination compound (Figure 1) presents a neutral complex featuring an approximately square planar geometry for the palladium center, which is bound to three pyrrolic nitrogen atoms and one adventitious water molecule. The hydrogen atoms on the aqua ligand engage in hydrogen-bonding interactions with the carbonyl groups of the tripyrrindione framework (O1–O3, 2.552 Å; O2–O3, 2.574 Å). The C–O distances (1.236–1.242 Å) on the pyrrolidone rings are consistent with double bonds and similar to those reported for bis-lactam H_3TD1,[26] thereby excluding the formation of a tautomeric lactim. In addition, the isolated tripyrrindione complex features Pd–N bond distances that are similar to those reported for Pd^{II} complexes of other linear oligopyrroles.[25,28] We therefore hypothesized the concomitant occurrence of metal coordination and one-electron oxidation of the ligand, which would coordinate as a dianionic radical (formally TD1$^{2-\bullet}$) rather than a trianionic diamagnetic species (TD1^{3-}).

The hypothesis of a ligand-based radical was confirmed by electron paramagnetic resonance (EPR) spectroscopy. The continuous-wave EPR spectrum of the complex recorded in toluene at room temperature (Figure 2) exhibits a single line centered at $g \approx 2.003$ (typical for organic radicals) and has a width of 0.59 mT. The spin concentration for this signal was quantified using the stable nitroxide radical 2,2,6,6-tetramethylpiperidin-1-yl)oxyl (TEMPO) as a reference. Within standard accuracy limits (estimated at ± 15%, see Supporting Information (SI) for details),[29] the spin concentration was found to be equivalent to the concentration of the dissolved complex and therefore consistent with a stable radical of formula [Pd^{II}(TD1•)(H_2O)].[30]

Single-point DFT calculations at the PBE0/ECP-(28MDF){Pd}q/def2-tzvp level of theory were performed following geometry optimization of [Pd(TD1•)(H_2O)] at the BP86 level of theory. The calculated frontier molecular orbitals (MOs) for the complex were found to be almost exclusively ligand-based (Figure 3). The SOMO for [Pd(TD1•)(H_2O)] is best described as a ligand(π)-Pd($4d_{yz}$) antibonding orbital with high ligand character and only 3.3% Pd character. Consistent with the observed EPR data, ca. 99% of the total unpaired spin density resides on the tripyrrindione ligand system, primarily on the C–C π-system of the two pyrrolidone rings (20.0% on each) and the central pyrrole (36.4%), with minor contributions from the carbonyl O($2p_y$) AOs (9.5% on each) and the N($2p_y$) AO (3.1%) *trans* to the aqua ligand. All experimental and computational findings therefore indicate that [Pd(TD1•)(H_2O)] is best described as a Pd^{II} complex with a TD1$^{2-\bullet}$ π-radical ligand.

The cyclic voltammogram of [Pd(TD1•)(H_2O)] in CH_2Cl_2 (Figure 4) exhibits a reduction at −0.672 V and an oxidation at −0.052 V relative to the ferrocene/ferrocenium couple (Fc/Fc$^+$). The ΔE_p values (80 mV for both events) and the linear

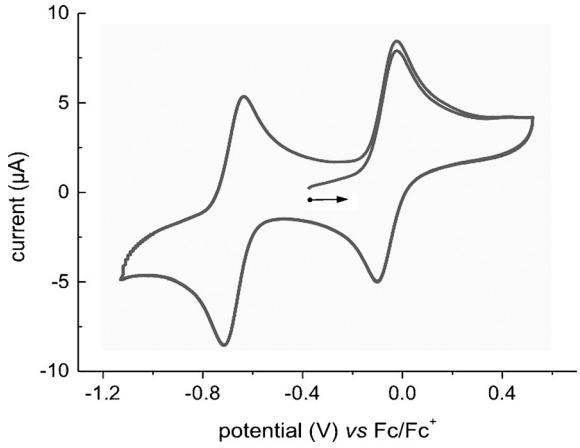

Figure 4. Cyclic voltammogram of [Pd(TD1•)(H$_2$O)] at a glassy carbon electrode in CH_2Cl_2 with (nBu$_4$N)(PF$_6$) as a supporting electrolyte. Data collected at a scan rate of 100 mV s^{-1} using a Ag/AgCl pseudo-reference electrode and a platinum wire auxiliary electrode.

relationship between measured current and square root of scan rate (Figure S5, SI) indicate that both processes are quasi-reversible one-electron events. By comparison, the cyclic voltammogram of the free ligand (Figure S6, SI) is complicated and presents at least three irreversible reduction events at potentials lower than −1.6 V and several oxidations above 0.1 V, including a quasi-reversible event at approximately 0.25 V.

The electrochemical profile of [Pd^{II}(TD1•)(H$_2$O)] prompted us to pursue its one-electron transformations (both reductive and oxidative) by chemical methods and to characterize the other oxidation states of the redox-active ligand platform. Following one-electron oxidation of [Pd^{II}(TD1•)(H$_2$O)] by stoichiometric $AgBF_4$, we isolated a species comprising the cationic complex [Pd(TD1)(H$_2$O)]$^+$ and the [BF$_4$]$^-$ counter ion (Figure 5, top panel). The ^{1}H NMR spectrum of this diamagnetic species shows the expected downfield shifts of resonances in comparison with the free ligand H$_3$TD1 (Figure S1, SI). Conversely, addition of 1 equiv of reductant CoCp*$_2$ (Cp* = pentamethylcyclopentadienyl) to a solution of [Pd^{II}(TD1•)(H$_2$O)] at room temperature under an inert atmosphere afforded a one-electron reduction product featuring the anionic tripyrrindione complex [Pd(TD1)(H$_2$O)]$^-$ and the cobaltocenium counter ion [CoCp*$_2$]$^+$ (Figure 5, bottom panel). Both one-electron redox events can be monitored by UV-vis spectrophotometry as they are accompanied by a shift of the main absorption features of [Pd^{II}(TD1•)(H$_2$O)] in the 550–650 nm region and by complete disappearance of two near-infrared bands at 826 and 933 nm (Figure S2, SI).

Consistent with the electrochemical data (Figure 4), the tripyrrindione ligand undergoes two changes in oxidation state with no significant changes in the planar geometry or bond distances of the Pd^{II} primary coordination sphere. As expected for ligand-based redox events, the largest alterations in bond distances (up to ± 0.04 Å) are observed on the ligand scaffold (Table S2, SI). In particular, the one-electron oxidation and reduction of [Pd^{II}(TD1•)(H$_2$O)] have opposite effects on bond distances (i.e., in bonds for which oxidation causes

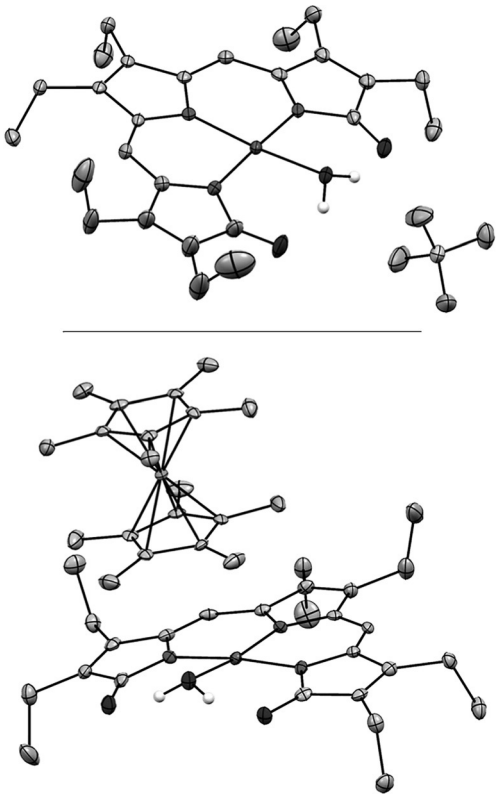

Figure 5. Crystal structure of complexes [Pd(TD1)(H$_2$O)][BF$_4$] (top) and [CoCp*$_2$][Pd(TD1)(H$_2$O)] (bottom). Carbon-bound hydrogen atoms in calculated positions are omitted for clarity. Thermal displacement ellipsoids are set at the 50% probability level (top: CCDC 1400991, bottom: CCDC 1400989).

lengthening, reduction causes shortening). DFT computational analyses (see SI for details) support closed-shell configurations for both oxidized and reduced complexes. Specifically, for the [Pd(TD1)(H$_2$O)]$^-$ complex, the singlet state is approximately 1.3 eV lower in energy when compared to the triplet state, and the doubly filled HOMO is a ligand-(π)-Pd(4d$_{yz}$) antibonding orbital with low Pd character (3.9%). Experimental and computational findings on the products of one-electron redox reactions are hence consistent with loss or gain of one electron from the same type of ligand-based MO.

This unique series of Pd^{II} complexes allows comparison of the hydrogen bonding interactions between the aqua ligand and the TD1 ligand system in three different redox states. The donor-acceptor distances decrease from the longest value (2.579 Å) in the cationic complex to the shortest one (2.521 Å) in the anionic complex (Table S3, SI). Conversely, the hydrogen-bonding angles (O–H···O) increase from a minimum of 143.49° in [Pd(TD1)(H$_2$O)]$^+$ to a maximum of 160.11° in [Pd(TD1)(H$_2$O)]$^-$. In both cases the parameters of the neutral complex lie in between those of the charged ones. The crystallographic parameters[31] therefore indicate that the hydrogen-bonding strength increases with the number of electrons on the tripyrrindione framework and hence is modulated by the redox state of the acceptor system. Electronic structure calculations are consistent with this

assessment. As $[Pd^{II}(TD1)(H_2O)]^+$ is reduced to $[Pd^{II}(TD1^{\bullet})(H_2O)]$ and then $[Pd^{II}(TD1)(H_2O)]^-$, the calculated strength of the hydrogen bond increases by $\sim 2\ kcal\,mol^{-1}$ for each one-electron reduction (Figure S10, SI).

One-electron oxidations of tetrapyrrolic bilindione have been observed upon coordination of several divalent transition metals, including Cu^{II}, Ni^{II} and Pd^{II},[9,25] which resulted in helical complexes featuring ligand-based radicals. Notably, the marked redox non-innocence of biliverdine analogs has been in part associated with the sterics of their curved π systems.[32] Our findings show that the smaller tripyrrindione scaffold not only stabilizes an unpaired electron at room temperature on its planar π system, but also offers a tridentate geometry suitable for access to the metal center for an additional in-plane ligand (i.e., H_2O in the case of $[Pd^{II}(TD1^{\bullet})(H_2O)]$). The influence on reactivity of the identity of the metal center and of the hydrogen-bonding interactions to the pyrrolidone carbonyl groups will be the focus of upcoming studies.

Known as a urinary pigment emerging from physiological pathways of heme degradation, the tripyrrindione fragment provides a stable platform for transition metal coordination and one-electron ligand-based redox chemistry. This pincer-type ligand, which we characterized in three different oxidation states, could offer the advantages of oligopyrroles (e.g., electron-rich scaffold, highly tunable redox properties) to modern catalytic applications employing redox non-innocent ligands.

Acknowledgements

We gratefully acknowledge Dr. Tsuhen M. Chang for assistance with synthetic procedures and Dr. Sue Roberts for assistance with the collection and analysis of X-ray diffraction data. This work was supported by the Donors of the American Chemical Society Petroleum Research Fund (grant 51754-DNI3 to E.T.) and by the National Science Foundation (CAREER grant 1454047 to E.T.). A.V.A. gratefully acknowledges NSF (DBI-0139459, DBI-9604939, and BIR-9224431) and NIH (S10RR020959 and S10RR026416-01) grants for the development of the EPR facility at the University of Arizona. J.S. acknowledges NSF for financial support (CHE-1362662).

Keywords: oligopyrroles · redox non-innocence · redox-active ligands · tripyrrindione · uroerythrin

How to cite: *Angew. Chem. Int. Ed.* **2015**, *54*, 14894–14897
Angew. Chem. **2015**, *127*, 15107–15110

[1] P. J. Chirik, K. Wieghardt, *Science* **2010**, *327*, 794–795.
[2] V. Lyaskovskyy, B. de Bruin, *ACS Catal.* **2012**, *2*, 270–279.
[3] O. R. Luca, R. H. Crabtree, *Chem. Soc. Rev.* **2013**, *42*, 1440–1459.
[4] R. Eisenberg, H. B. Gray, *Inorg. Chem.* **2011**, *50*, 9741–9751.
[5] M. Stillman, *J. Porphyrins Phthalocyanines* **2000**, *4*, 374–376.
[6] P. Schweyen, K. Brandhorst, R. Wicht, B. Wolfram, M. Bröring, *Angew. Chem. Int. Ed.* **2015**, *54*, 8213–8216; *Angew. Chem.* **2015**, *127*, 8331–8334.
[7] S. Ye, T. Tuttle, E. Bill, L. Simkhovich, Z. Gross, W. Thiel, F. Neese, *Chem. Eur. J.* **2008**, *14*, 10839–10851.
[8] F. A. Walker, S. Licoccia, R. Paolesse, *J. Inorg. Biochem.* **2006**, *100*, 810–837.
[9] A. L. Balch, M. Mazzanti, B. C. Noll, M. M. Olmstead, *J. Am. Chem. Soc.* **1993**, *115*, 12206–12207.
[10] A. L. Balch, M. Mazzanti, B. C. Noll, M. M. Olmstead, *J. Am. Chem. Soc.* **1994**, *116*, 9114–9122.
[11] L. K. Blusch, K. E. Craigo, V. Martin-Diaconescu, A. B. McQuarters, E. Bill, S. Dechert, S. DeBeer, N. Lehnert, F. Meyer, *J. Am. Chem. Soc.* **2013**, *135*, 13892–13899.
[12] C. M. Davis, K. Ohkubo, I. T. Ho, Z. Zhang, M. Ishida, Y. Fang, V. M. Lynch, K. M. Kadish, J. L. Sessler, S. Fukuzumi, *Chem. Commun.* **2015**, *51*, 6757–6760.
[13] M. Ishida, J.-Y. Shin, J. M. Lim, B. S. Lee, M.-C. Yoon, T. Koide, J. L. Sessler, A. Osuka, D. Kim, *J. Am. Chem. Soc.* **2011**, *133*, 15533–15544.
[14] H. Rath, S. Tokuji, N. Aratani, K. Furukawa, J. M. Lim, D. Kim, H. Shinokubo, A. Osuka, *Angew. Chem. Int. Ed.* **2010**, *49*, 1489–1491; *Angew. Chem.* **2010**, *122*, 1531–1533.
[15] Y. Hisamune, K. Nishimura, K. Isakari, M. Ishida, S. Mori, S. Karasawa, T. Kato, S. Lee, D. Kim, H. Furuta, *Angew. Chem. Int. Ed.* **2015**, *54*, 7323–7327; *Angew. Chem.* **2015**, *127*, 7431–7435.
[16] A. Kochem, L. Chiang, B. Baptiste, C. Philouze, N. Leconte, O. Jarjayes, T. Storr, F. Thomas, *Chem. Eur. J.* **2012**, *18*, 14590–14593.
[17] M. Bröring in *Handbook of Porphyrin Science*, *Vol. 8* (Eds.: K. M. Kadish, K. M. Smith, R. Guilard), World Scientific, Singapore, **2010**, pp. 343–485.
[18] M. Bröring, C. D. Brandt, *Chem. Commun.* **2001**, 499–500.
[19] J. L. Sessler, A. Gebauer, V. Král, V. Lynch, *Inorg. Chem.* **1996**, *35*, 6636–6637.
[20] A. Jaumà, J.-A. Farrera, J. M. Ribo′, *Monatsh. Chem.* **1996**, *127*, 935–946.
[21] G. Park, J. T. Tomlinson, M. S. Melvin, M. W. Wright, C. S. Day, R. A. Manderville, *Org. Lett.* **2003**, *5*, 113–116.
[22] T. M. Chang, S. Sinharay, A. V. Astashkin, E. Tomat, *Inorg. Chem.* **2014**, *53*, 7518–7526.
[23] J. Beruter, J. P. Colombo, U. P. Schlunegger, *Eur. J. Biochem.* **1975**, *56*, 239–244.
[24] T. Yamaguchi, I. Shioji, A. Sugimoto, Y. Komoda, H. Nakajima, *J. Biochem.* **1994**, *116*, 298–303.
[25] P. A. Lord, M. M. Olmstead, A. L. Balch, *Inorg. Chem.* **2000**, *39*, 1128–1134.
[26] S. D. Roth, T. Shkindel, D. A. Lightner, *Tetrahedron* **2007**, *63*, 11030–11039.
[27] S. K. Dey, S. Datta, D. A. Lightner, *Monatsh. Chem.* **2009**, *140*, 1171–1181.
[28] M. Bröring, C. D. Brandt, *J. Chem. Soc. Dalton Trans.* **2002**, 1391–1395.
[29] G. Casteleijn, J. J. ten Bosch, J. Smidt, *J. Appl. Phys.* **1968**, *39*, 4375–4380.
[30] Possibly owing to stacking interactions, the measured spin concentration appears lower in frozen solutions. This effect is reversible and the signal is fully restored upon warming to room temperature (see SI for details).
[31] T. Steiner, *Angew. Chem. Int. Ed.* **2002**, *41*, 48–76; *Angew. Chem.* **2002**, *114*, 50–80.
[32] I. Wasbotten, A. Ghosh, *Inorg. Chem.* **2006**, *45*, 4914–4921.

Received: August 5, 2015
Published online: October 8, 2015

